FULL PAPER

Synthesis and Characterization of New Thieno[3,4-c] pyrrole-4,6-dione Derivatives for Photovoltaic Applications

*Ahmed Najari, Serge Beaupré, Philippe Berrouard, Yingping Zou, Jean-Rémi Pouliot, Charlotte Lepage-Pérusse, and Mario Leclerc**

A new class of low-bandgap copolymers based on benzodithiophene (BDT) and thieno[3,4-c]pyrrole-4,6-dione (TPD) units is reported. Chemical modifications of the conjugated backbone promote both high molecular weights and processability while allowing for tuning of the electronic properties. Copolymers with substituted thiophene spacers (alkyl chains facing the BDT unit) or unsubstituted thiophene spacers tend to have low power conversion efficiencies (PCE less than 1%) due to a bad morphology of the active layer, whereas copolymers with substituted thiophene spacers (alkyl chains facing TPD unit) show enhanced morphology and PCEs up to of 3.9%. Finally, BDT-TPD copolymers without any thiophene spacers still show the best performances with power conversion efficiencies up to 5.2%.

1. Introduction

Harvesting the unlimited and renewable energy from sunlight to produce electricity through photovoltaic devices is a promising way to address growing global energy needs while minimizing detrimental effects on the environment. Among all photovoltaic technologies, polymer bulk heterojunction (BHJ) solar cells offer a compelling option for tomorrow's photovoltaic devices since they can be easily prepared using low-cost and energy efficient roll-to-roll manufacturing processes.[1–3] During the past decade, BHJ solar cells based on regioregular poly(3-hexylthiophene) (P3HT) and [6,6]-phenyl C61-butyric acid methyl ester ([60]PCBM) blend have been widely investigated and power conversion efficiencies (PCEs) up to 5–6% have been reported.[4–6] However, a relatively large bandgap of 1.9 eV and a highest occupied molecular orbital (HOMO) energy level of 5.1 eV prevent P3HT/PCBM-based BHJ solar cells from reaching higher PCE values.[7] Numerous studies on BHJ photovoltaic devices led to a widely accepted guideline for the design of new conjugated polymers used as donor in BHJ solar cells.[8,9] Indeed, when combined with the mostly used electron acceptor [60]PCBM, the donor should have a bandgap between 1.2 and 1.9 eV with broad absorption to match the spectral flux, a HOMO energy level between −5.2 and −5.8 eV and a lowest unoccupied molecular orbital (LUMO) energy level between −3.7 and −4.0 eV to ensure efficient charge separation while maximizing the open circuit voltage (V_{oc}). The past few years have witnessed the development of several new classes of conjugated polymers that have been used as donors in BHJ solar cells.[10–12] Lately, PCEs up to 8.1% have been reported, which confirms that organic photovoltaic technology can become a cost-effective and competitive technology.[13]

Recently, we have reported for the first time a new class of copolymers based on benzodithiophene (BDT) and thieno[3,4-c]pyrrole-4,6-dione (TPD).[14] The TPD unit is attractive due its compact planar structure that could be beneficial to the electron delocalization when incorporated into various conjugated polymers. Moreover, it seems that it should promote intra- and interchain interactions along and between coplanar polymer chains and its strong electron-withdrawing effect should lead to lower HOMO and LUMO energy levels, a desired property to increase the stability and the V_{oc} in BHJ solar cells. Furthermore, TPD can be easily prepared in few steps from commercially available compounds. A PCE of 5.5% was obtained using a poly((4,8-diethylhexyloxyl) benzo[1,2-b:4,5-b']dithiophene)-2,6-diyl)-alt-((5-octylthieno[3,4-c]pyrrole-4,6-dione)-1,3-diyl) (PBDTTPD)/[70]PCBM blend for an active area of 100 mm^2.[14] Following this paper, several research groups confirmed that copolymers based on BDT and TPD units can reach high power conversion efficiencies. Jen et al.[15] reported power conversion efficiency of 4.1% for PBDTTPD/[70]PCBM (ratio 1:2) while Fréchet et al.[16] and Xie et al.[17] reported PCEs ranging from 4.0% to 6.8% for a series of alkylated TPD-based copolymers. Recently, Wei et al.[18] reported a power conversion efficiency of 4.7% with a high V_{oc} of 0.95 V using a copolymer based on TDP and bithiophene derivatives.

Following these first studies on copolymers based on BDT and TPD units (**Figure 1**), we report the syntheses and the characterization of new copolymers based on BDT and alkylated-TPD comonomers where thiophene spacers were added to tune the electronic properties and to enhance photons harvesting. Effects on the morphology and phase separation using these new copolymers were also investigated using grazing incidence X-ray scattering (GIXS) and atomic force microscopy (AFM).

Dr. A. Najari, Dr. S. Beaupré, P. Berrouard, Dr. Y. Zou,
J.-R. Pouliot, C. Lepage-Pérusse, Prof. M. Leclerc
Canada Research Chair on Electroactive and Photoactive Polymers
Department of Chemistry
Université Laval
Quebec City, Quebec, G1V 0A6, Canada
E-mail: Mario.Leclerc@chm.ulaval.ca

DOI: 10.1002/adfm.201001771

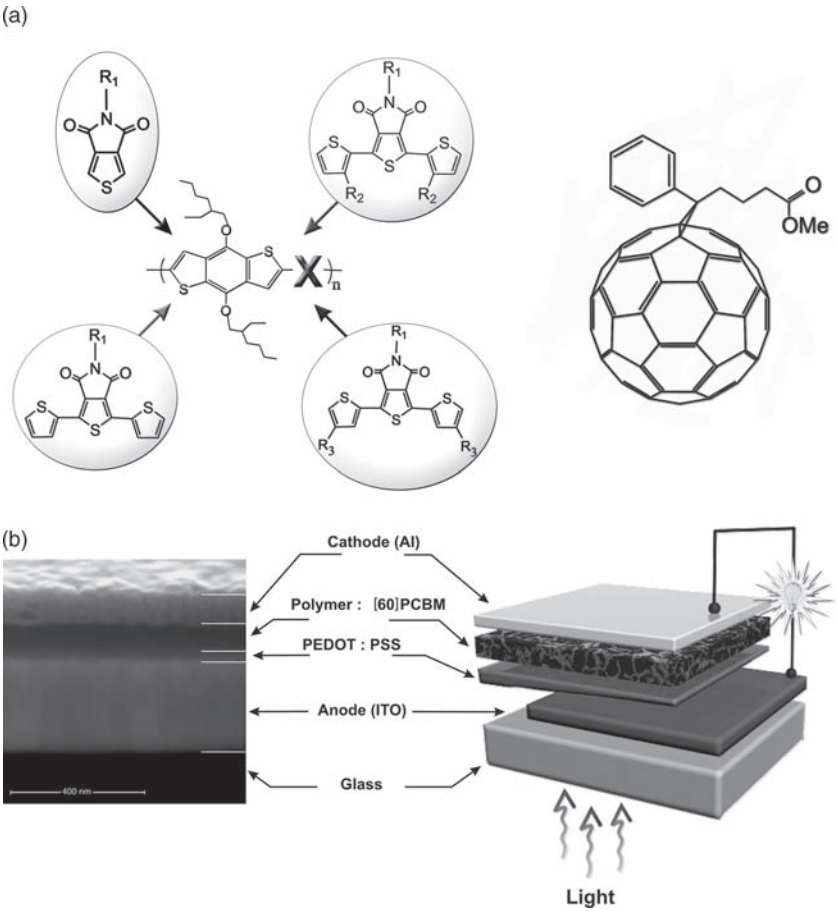

Figure 1. a) Molecular structures of the active materials: poly(thieno[3,4-c]pyrrole-4,6-dione) derivatives (left) and [60]PCBM (right). b) The device structure (left) and scanning electron microscopy (SEM) cross-sectional image (right) of the polymer solar cell.

Since the thickness of the active layer may be a critical issue for a reliable roll-to-toll processing of BHJ solar cells, both thin and thick active layers were investigated using a 25 mm^2 active area.

2. Results and Discussion

2.1. Monomers and Copolymers

The synthetic routes for comonomers are shown in **Scheme 1** and **Scheme 2**. Our work on BDT-TPD copolymers (not reported here) and other studies on BDT-based copolymers have shown that benzo[1,2-b:3,4-b]dithiophene (BDT) bearing ethylhexyl side chain led to soluble copolymers with high molecular weights, enhanced morphology for films obtained from copolymer/[60]PCBM blends, and high power conversion efficiency in BHJ solar cells.[14–17,19] Since alkyl side chains on the TPD unit can also influence the solubility, the molecular weights, the organization, and the charge mobility of BDT-TPD copolymers, we have investigated the influence of the alkyl chains of the TPD unit (**P1–P3**) on the morphology of the copolymer/[60]PCBM blend.

The synthesis of comonomers **4–6** was straightforward and proceeded in good yields according to reported procedures.[20] The Stille coupling between comonomers **4–6** and BDT comonomer gave soluble copolymers with moderate molecular weights (**P1–P3**) (**Scheme 3**). In order to modulate the electronic properties and bandgap of BDT-TPD-based copolymers, an alkylated-TPD unit bearing on each side a thiophene unit (comonomers **19–26**) was also prepared. Unfortunately, copolymers with unsubstituted thiophene spacers and straight alkyl chains on the TPD unit (**P4**,**P6**) were found to be insoluble in most common organic solvents and could not be characterized. However, the use of a branched chain (ethylhexyl group) on the TPD unit led to a soluble and processable copolymer with moderate molecular weights (**P5**). Finally, **P7–P11** were prepared to investigate the influence of the length and of the positioning of alkyl chains on thiophene spacers on the solubility; molecular weights; and optical, electronic, and morphological properties.

It is worth noting that during the synthesis of precursors **11–18**, some by-products that indicate a side reaction involving a dimerization of the TPD unit (compounds **4–6**) were isolated. This side reaction might occur during the preparation of copolymers **P1–P3** and might lead to an imperfect alternating structure. The presence and the amount of these possible structural defects are under investigation.

2.2. Molecular Weights and Thermal Properties

All polymers were characterized by size exclusion chromatography (SEC) using monodisperse polystyrene standard in

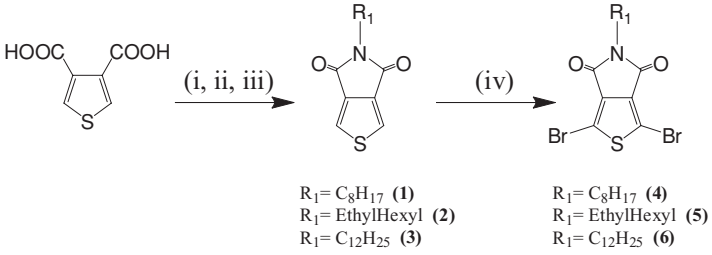

Reagents and conditions: (i)Ac_2O, 140°C, overnight; (ii) 1-octylamine or 2-ethyl-1-hexylamine or 1-dodecylamine, toluene, reflux 24h; (iii) $SOCl_2$, reflux, 12h, (iv) H_2SO_4, CF_3COOH, NBS, r.t., overnight.

Scheme 1. Synthesis of TPD precursors.

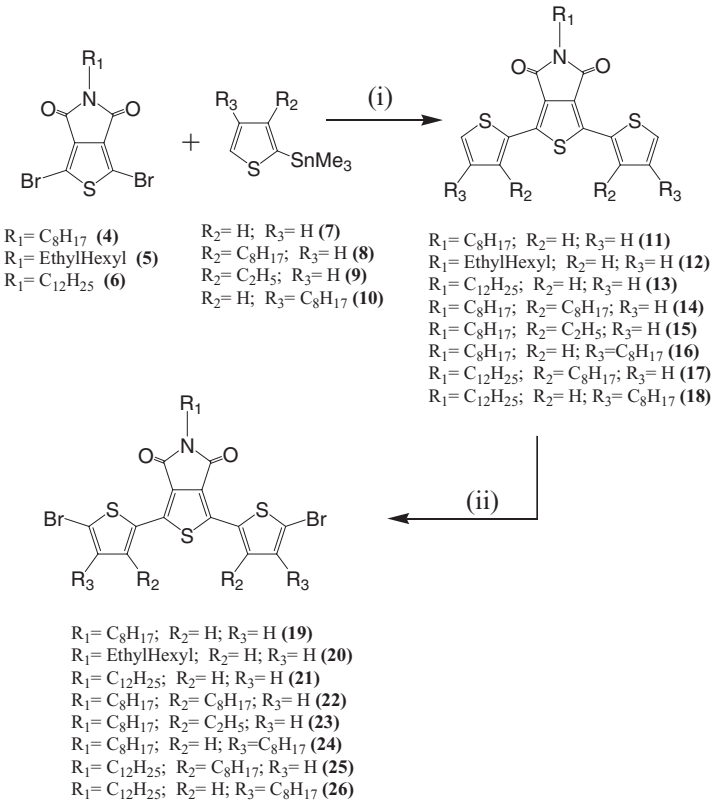

R_1= C_8H_{17} **(4)**
R_1= EthylHexyl **(5)**
R_1= $C_{12}H_{25}$ **(6)**

R_2= H; R_3= H **(7)**
R_2= C_8H_{17}; R_3= H **(8)**
R_2= C_2H_5; R_3= H **(9)**
R_2= H; R_3= C_8H_{17} **(10)**

R_1= C_8H_{17}; R_2= H; R_3= H **(11)**
R_1= EthylHexyl; R_2= H; R_3= H **(12)**
R_1= $C_{12}H_{25}$; R_2= H; R_3= H **(13)**
R_1= C_8H_{17}; R_2= C_8H_{17}; R_3= H **(14)**
R_1= C_8H_{17}; R_2= C_2H_5; R_3= H **(15)**
R_1= C_8H_{17}; R_2= H; R_3=C_8H_{17} **(16)**
R_1= $C_{12}H_{25}$; R_2= C_8H_{17}; R_3= H **(17)**
R_1= $C_{12}H_{25}$; R_2= H; R_3= C_8H_{17} **(18)**

R_1= C_8H_{17}; R_2= H; R_3= H **(19)**
R_1= EthylHexyl; R_2= H; R_3= H **(20)**
R_1= $C_{12}H_{25}$; R_2= H; R_3= H **(21)**
R_1= C_8H_{17}; R_2= C_8H_{17}; R_3= H **(22)**
R_1= C_8H_{17}; R_2= C_2H_5; R_3= H **(23)**
R_1= C_8H_{17}; R_2= H; R_3=C_8H_{17} **(24)**
R_1= $C_{12}H_{25}$; R_2= C_8H_{17}; R_3= H **(25)**
R_1= $C_{12}H_{25}$; R_2= H; R_3= C_8H_{17} **(26)**

Reagents and conditions: (i) $PdCl_2(PPh_3)_2$, THF, reflux, 24h; (ii) NBS, acetic acid, chloroform, 50°C, 24 h.

Scheme 2. Synthesis of TPD derivatives with flanked thiophene.

hot 1,2,4-trichlorobenzene (TCB) and data are summarized in **Table 1**. The number average molecular weight (M_n) ranges from 8.3 kDa to 131 kDa with a polydispersity index (PDI) between 1.5 and 3.2. Recently, Fréchet et al.[16] have reported higher number-average molecular weight for **P1** (M_n = 35 kDa; PDI = 2.7). Xie et al.[17] have also reported higher molecular weights for similar BDT-TPD copolymers with high polydispersity indexes. In both cases, the SEC measurements were carried out in tetrahydrofuran (THF). In order to adequately compare the molecular weights, SEC measurements in THF were attempted for **P1**. However, the **P1** sample was only slightly soluble in THF and the number-average molecular weight obtained for the soluble fraction was low (M_n < 5 kDa). Since **P1** was soluble in chloroform, SEC measurements in chloroform were also performed and a broad molecular weight distribution, which was attributed to aggregation, was found. This aggregation led to an overestimation of the apparent molecular weights and high polydispersity indexes.

Thermogravimetric analyses (TGA) showed that all polymers were thermally stable with degradation temperatures (T_d) ranging from 330 to 380 °C. With the exception of **P1** (T_g = 138 °C), differential scanning calorimetry (DSC) performed on **P2–P11** did not reveal any noticeable glass transition temperatures. Similar observations have been reported by Xie et al.[17]

2.3. Optical and Electrochemical Properties

The optical properties of all copolymers are summarized in Table 1. For all polymeric materials, the absorption spectra are broad, which means that a large part of the solar spectral flux will be absorbed (**Figure 2**) and should contribute to get high short circuit current (J_{sc}) in BHJ solar cells. One can see that the absorption spectra of **P1–P5** remain almost the same in solution and films (Figure 2b). Density functional theory (DFT) calculations performed on the **P1–P3** repeating units revealed coplanar structures (data not shown). Indeed, Wei et al.[18] reported that the electron-deficient TPD moiety exhibits a symmetric, rigidly fused, and coplanar structure. Moreover, neither the length nor the type of the tail chain on the TPD seems to affect the optical properties of these copolymers. Absorption spectrum of film of **P5** showed that the thiophene spacers (without alkyl chains) did not modulate the optical properties and the optical bandgap remains the same as **P1–P3**. In order to obtain soluble and high molecular weights BDT-TPD derivatives with thiophene spacers, copolymers **P7–P11** were prepared. For these copolymers, significant red shifts (up to 40 nm for **P8**) were observed when comparing solution to films. This typical behavior observed in dense thin-films of conjugated polymers is related to an increase in conjugation length due to an ordering in the solid state. However, the absorption spectra of these copolymers were blue shifted when compared to **P1–P3** but again the optical bandgap remained almost the same. One can see that only a small range of the optical bandgap (onset of the absorption spectra) was obtained for BDT-TPD derivatives meaning that the influence of thiophene spacer on the optical properties is somehow limited.

Cyclic voltammetry was utilized to evaluate the HOMO and LUMO energy levels as well as the bandgap of BDT-TPD derivatives. These data are summarized in Table 1 and **Figure 3**. The HOMO energy levels were estimated by using the onset of the oxidation potential (where the current differs from the baseline) from the first scan since all polymers showed non-reversible oxidation processes. On the other hand, all polymers showed reversible reduction processes and LUMO energy levels were also estimated the same way as HOMO energy levels. As observed for optical properties, the alkyl chain on the TPD unit did not dramatically change the electronic properties. Here, the relatively deep HOMO energy levels should contribute to obtain high V_{oc} in BHJs while the LUMO levels are within the desirable range for proper electron transfer from the donor to the electron acceptor ([60]PCBM).[8,9]

2.4. Photovoltaic Properties

The photovoltaic properties of copolymers **P1–P11** were investigated in BHJ solar cells using the following configura-

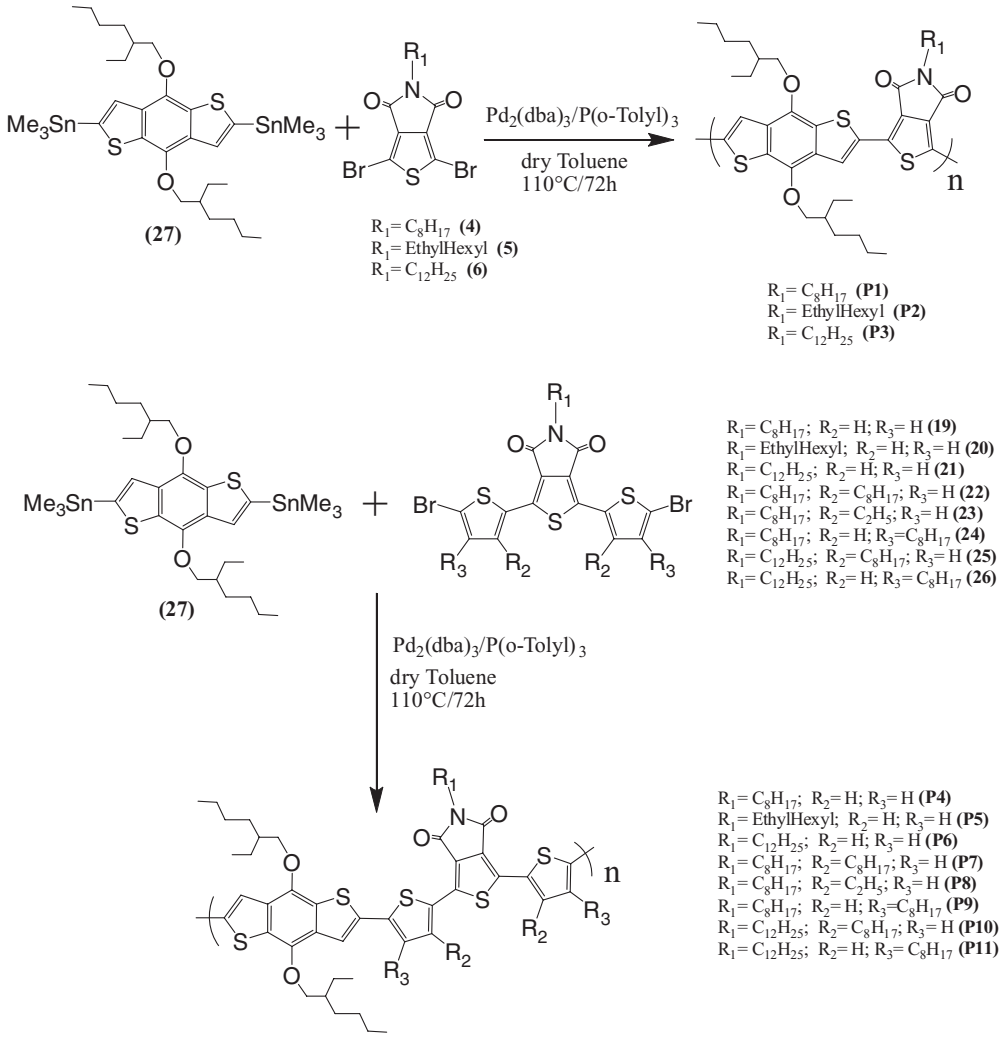

Scheme 3. Synthesis of poly(thieno[3,4-c]pyrrole-4,6-dione) derivatives.

Table 1. Molecular weights and optical and electrochemical properties of copolymers P1 to P11.

Polymer	M_n	PDI	T_d	Solution λ_{max}	Film λ_{max}	E_{HOMO}	E_{LUMO}	E_g^{cv}	E_g^{opt}
	(kDa)		(°C)	(nm)	(nm)	(eV)	(eV)	(eV)	(eV)
P1	12.0	2.37	380	308, 360, 448, 614	308, 360, 448, 614	−5.56	−3.75	1.81	1.80
P2	20.6	2.56	340	447, 556, 609	444, 555, 609	−5.66	−3.87	1.79	1.84
P3	16.1	2.23	330	555, 610	556, 615	−5.60	−3.82	1.78	1.84
P4[a)]	—	—	—	—	—	—	—	—	—
P5	8.3	1.50	330	512	516	−5.49	−3.70	1.65	1.84
P6[a)]	—	—	—	—	—	—	—	—	—
P7	131.0	2.82	340	524	539	−5.56	−3.70	1.86	1.88
P8	11.6	3.19	340	513	553	−5.54	−3.78	1.76	1.84
P9	19.9	2.11	330	517	539	−5.66	−3.83	1.83	1.86
P10	41.6	2.27	340	512	540	−5.56	−3.70	1.86	1.88
P11	22.9	2.30	330	519	538	−5.73	−3.78	1.95	1.89

[a)]P4 and P6 were not soluble.

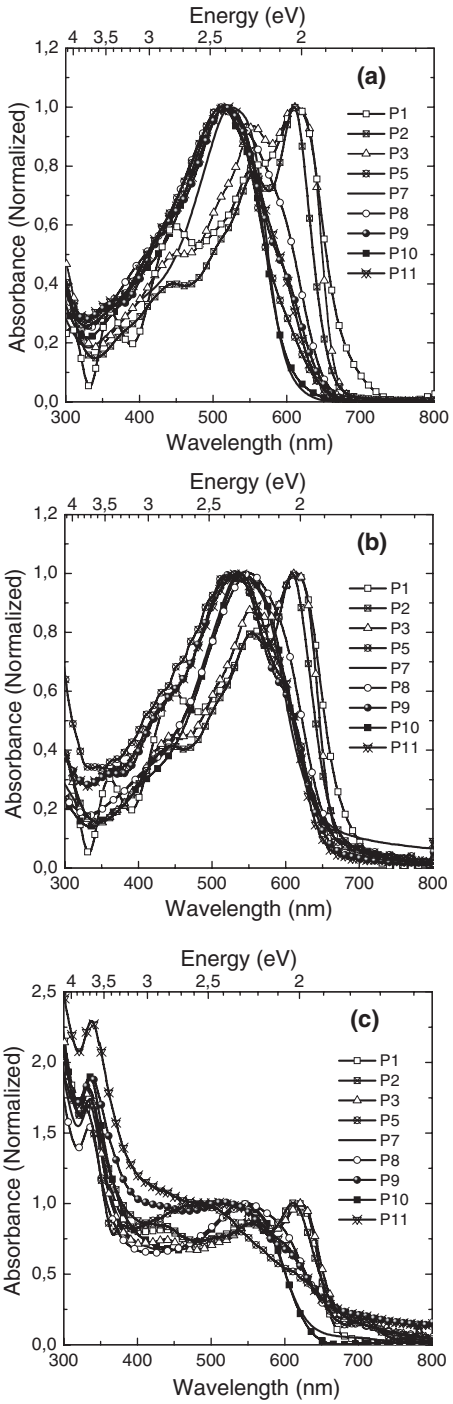

Figure 2. a) Normalized absorption spectra of TPD derivatives for dilute ortho-dichlorobenzene (oDCB) solutions for P1–P5, P8; for dilute chloroform solutions of P7, P10, and P11. **b)** In film. **c)** Films from copolymer/[60]PCBM blends.

tion: glass/indium tin oxide (ITO)/poly(3,4-ethylenedioxythiophene):poly(styrenesulfonate) (PEDOT:PSS)/active layer/Al (Figure 1). The active layer was a blend of **P1**–**P11** with [60]PCBM spin-coated from chloroform or oDCB solutions. For **P1** and **P10**, both thin and relatively thick active layers were prepared. The ratio of donor:acceptor was optimized and found to be 1:2 (wt:wt) for all polymers, excepted for **P2** (1:1). Solar cells were tested under AM 1.5G (AM = air mass) illumination of 100 mW cm^{-2} and the active area of the devices was 25 mm^2 (**Table 2**). Current density–voltage (*J*–*V*) curves are shown in **Figure 4** and data on BHJ solar cells are summarized in Table 2.

Based upon the equivalent circuit of a photovoltaic cell,[21,22] the current vs voltage (*I*–*V*) characteristics can be described by the following equation:[21,23]

$$I = I_0 \left[\exp\left(e\frac{V - I R_S}{nkT} \right) - 1 \right] + \frac{V - I R_S}{R_{sh}} - I_{ph} \quad (1)$$

where I_0 is the dark current, e is the electron charge, n is the diode ideality factor, V is the applied voltage, R_s is the series resistance, R_{sh} is the shunt resistance, and I_{ph} is the photocurrent. R_s and R_{sh} can be described by the following equations.[24]

$$\left[\frac{dI}{dV}\right]_{I=0} \approx R_S^{-1} \quad (2)$$

$$\left[\frac{dI}{dV}\right]_{V=0} \approx R_{sh}^{-1} \quad (3)$$

Thus, to obtain high short-circuit currents, I_{sc} ($V = 0$), solar cell devices must have small R_s and large R_{sh}. In a physical point of view, the series resistance R_s can be associated with the materials' conductivity, thus the charge carrier mobility in the donor/acceptor (D/A) blends (electron mobility in the acceptor and hole mobility in the donor). R_{sh} interprets the charge recombination close to dissociation charge sites (interface D/A and electrodes).

According to reported data, **P1** and **P3** show the best photovoltaic performances with high V_{oc} (0.94 V and 0.96 V, respectively) and J_{sc} of 10.8 mA cm^{-2} and 10.0 mA cm^{-2}, respectively. Moderate fill factors (FFs), approaching 51% for both copolymers, led to PCEs of 5.2% for **P1** and 4.8% for **P3** (thin films). Fréchet et al.[16] reached a PCE up to 6.3% for **P1** (with M_n = 35 kDa) in BHJ solar cells and Jen et al.[15] have reported a PCE up to 4.1% for **P1** for devices using [70]PCBM. These high PCEs underline a significant potential of this copolymer in organic solar cells applications. Since high-speed roll-to-roll manufacturing process can be used to print polymeric solar cells,[25] the use of relatively thick films is important in order to obtain a uniform and defect free active layer. **P1** is a promising material that could fulfill those requirements. Indeed, we obtained BHJ solar cells with a PCE up to 3.8% using an active layer with a thickness of 170 nm. While the V_{oc} and J_{sc} remain almost the same when compared to thin films devices, the *FF* drops by more than 20%. This can be attributed to the low mobility of holes for **P1** ($\mu_h = 1.6 \times 10^{-4}$ cm^2 V^{-1} s^{-1}), which increase R_s and decrease R_{sh} for thicker films. Despite this fact, the PCE reported here for **P1** is among the highest values reported in literature for thick-layer BHJ solar cells. According to data reported in Table 2, the length of the alkyl on the TPD unit (from octyl to docecyl) led to a lower PCE (4.8%), caused by a drop of J_{sc} even though R_{sh} was higher for **P3** (1163 Ω cm^2)

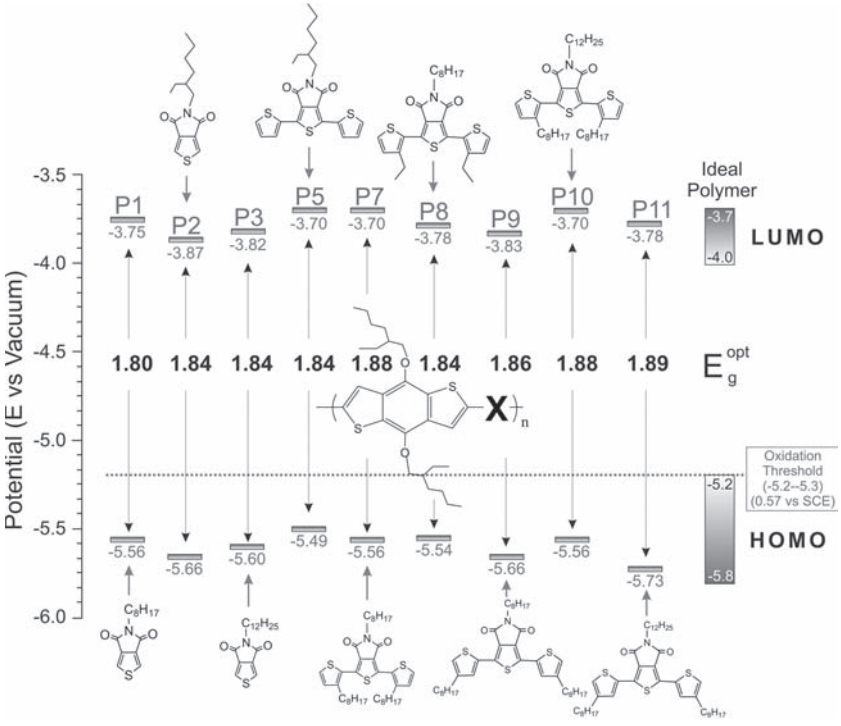

Figure 3. Energy levels of copolymers P1 to P11.

than for **P1** (994 Ω cm^2). Fréchet et al.[16] and Xie et al.[17] have reported similar PCEs with **P2.**

The BDT-TPD derivatives with thiophene spacers with alkyl chains facing the TPD unit also revealed promising photovoltaic results (**P7**, **P8**, and **P10**). Among these copolymers, the high molecular weight copolymer **P7** gave the best photovoltaic results with a PCE of 3.9% (thickness of 102 nm). **P10** (with $C_{12}H_{25}$ on the TPD unit) reached a PCE of 3.6% with an V_{oc} of 0.87 V and a *FF* of 58%. Data reported in Table 2 clearly show that devices using **P7** are better than ones using **P8** and **P10** due to a higher shunt resistance value (R_{sh} = 1904 Ω cm^2). For **P10**, a lower shunt resistance causes power losses in solar cells by providing an alternate current path for the light-generated current. However, when used in a thick-film configuration (165 nm), **P10** shows a high V_{oc} (0.88 V) and a PCE of 3.1%. As for **P1** and **P3**, the length of the alkyl chain causes a small drop in the short circuit current J_{sc}, probably due to the morphology of the blend with the [60]PCBM. **P8** was prepared to obtain soluble copolymers with the shortest alkyl chain on the thiophene space since **P4** and **P6** were insoluble in most common organic solvents. Despite a high J_{sc} of 9.0 mA cm^{-2}, a drop in the V_{oc} of 0.23 V led to a PCE of 3.5%. Finally, the BDT-TPD derivatives with thiophene spacer bearing alkyl chains facing the BDT unit gave the worst results with PCEs of 0.2% and 0.7% for **P9** and **P11**, respectively. For both copolymers, the values of the J_{sc} and *FF* were low and are easily explained by the nanoscale morphology observed using AFM. While the nanoscale morphology of blends of **P1–P5**,**P7**, **P8**, and **P10** with [60]PCBM are quite similar with only small variations of the roughness nanoscale surface, morphologies of blends for **P9** and **P11** were completely different. As shown in **Figure 5**, "donut" shapes with a diameter of 500 nm were observed. The percolation pathways were poorly formed, which limits the transport of the charges to the respective electrodes and leads to poor short circuit current. To confirm these assump-

Table 2. Device Characteristics of Photovoltaic solar cells based on TPD containing Polymers with [60]PCBM.

Polymer	Solvent	D:A Ratio	J_{sc}	V_{oc}	FF	PCE	R_s	R_{sh}	Active Layer Thickness
		(wt:wt)	(mA cm^{-2})	(V)		(%)	(Ω cm^2)	(Ω cm^2)	(nm)
P1	oDCB	1:2	−10.8	0.94	0.51	5.2	18	994	98
	oDCB	1:2	−10.2	0.92	0.41	3.8	30	407	170
P2	oDCB	1:1	−6.2	0.96	0.43	2.6	52	480	67
P3	oDCB	1:2	−10.0	0.93	0.51	4.8	23	1163	95
P4[a)]	–	–	–	–	–	–	-	–	–
P5	oDCB	1:2	−2.9	0.76	0.43	0.95	61	884	88
P6[a)]	–	–	–	–	–	–	–	–	–
P7	$CHCl_3$	1:2	−7.6	0.89	0.57	3.9	19	1904	102
P8	oDCB	1:2	−9.0	0.76	0.51	3.5	20	700	70
P9	$CHCl_3$	1:2	−1.2	0.66	0.26	0.2	690	1222	115
P10	$CHCl_3$	1:2	−7.2	0.87	0.58	3.6	19	533	90
	CHC_3	1:2	−6.5	0.88	0.53	3.1	32	958	165
P11	$CHCl_3$	1:2	−2.3	0.92	0.34	0.7	97	772	85

[a)]P4 and P6 are not soluble.

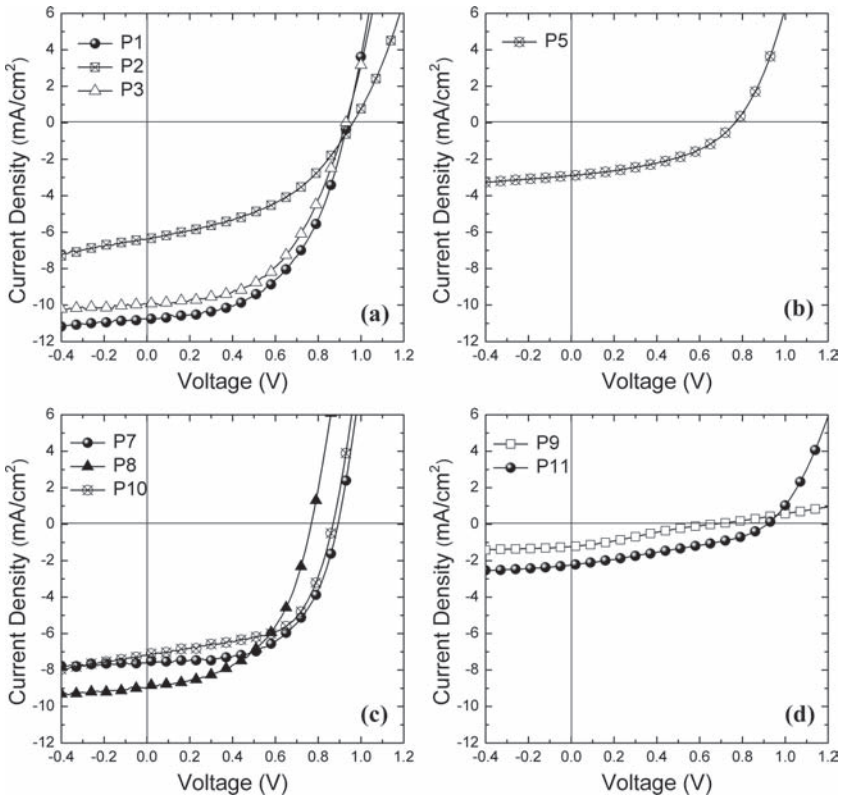

Figure 4. *J–V* curves of the polymers solar cells based on poly(thieno[3,4-c]pyrrole-4,6-dione) derivatives under the illumination of AM 1.5, 100 mW cm^{-2}. a) Polymers without thiophene spacer, b) polymers with thiophene spacer, c) polymers with thiophene spacer having alkyl chains facing TPD unit, and d) polymers with thiophene spacer having alkyl chains facing BDT unit.

tions, we investigated the influence of alkyl chains on the TPD unit (**P1–P3**) and also the influence of the thiophene spacers (**P5**, **P7–P11**) on the molecular organization in polymer thin films using GIXS. **P1–P3**, **P5**, **P7–P11**/[60]PCBM GIXS analyses were conducted on glass/ITO/PEDOT:PSS solid support. As shown in **Figure 6** , a peak at 4.2 Å, has been observed for all copolymers/[60]PCBM blends. This peak corresponds to the distance between the coplanar π-conjugated backbones (d_2). Indeed, Fréchet et al.[16] have reported smaller π-stacking distances for blends of **P1** (d_2 = 3.6 Å) and **P2** (d_2 = 3.8 Å) with [60]PCBM. According to the authors,[16] the fact that the π-stacking peak was observed for the entire BDT-TPD series indicating that these copolymers are able to retain the same face-on orientation when blended with the electron acceptor ([60]PCBM). For **P1–P3**, one can see an additional peak that corresponds to lamellar spacing (d_1). Since this distance is related to the length of the side chain, it is longer for the dodecyl derivative **P3** (d_1 = 24.6 Å) than the octyl derivative **P1** (d_1 = 21.2 Å) and ethylhexyl derivative **P2** (d_1 = 18.6 Å). These results are in good agreement with those reported by Fréchet et al.[16] These peaks were also present for **P8** (d_1 = 17.3 Å) and **P10** (d_1 = 20.6 Å). One can think that the shorter distance observed for **P8** (ethyl on the thiophene spacer) led to a better order in the blend, which led to higher J_{sc} (9.0 mA cm^{-2}) in BHJ solar cells when compared to **P10** (J_{sc} = 7.2 mA cm^{-2}). On the other hand, while **P7** gave a better power conversion efficiency with 3.9%, the GIXS diffractogram did not show any lamellar distance related peak as for the less efficient BDT-TPD derivatives (**P5**, **P9**, and **P11**).

In brief, copolymers with substituted thiophene spacers (alkyl chains facing the BDT unit) or the ones with unsubstituted thiophene spacers have the lower performances due to a poor morphology of the active layer. Indeed the "donut" shapes observed in AFM measurements for polymers **P9** and **P11** suggest poor charge transport properties due to a poor percolation in the polymer/[60]PCBM blends. Moreover, unlike other copolymers in the series, GIXS measurements did not reveal the presence of a peak around 20 Å, which is usually attributed to lamellar spacing. In addition to its lack of solubility in oDCB, **P5** shows low PCEs (less than 1%) due to a weak interpenetrated network of the donor and the acceptor. It is important to note that the carrier lifetime is largely controlled by the phase morphology between the donor and acceptor materials.[10] Furthermore, the molecular weight for this polymer is rather low at 12.5 kDa. As for **P1–P3**, AFM and GIXS measurements of copolymers (**P7**, **P8**, **P10**) show suitable film morphology that could lead to high PCE. It is noteworthy that the photovoltaic properties of this new class of materials have been obtained without any optimization processes. According to the tool proposed by the Konarka Technologies Inc. team,[9] it seems that a PCE up to 8.5% can be reached using this new class of materials so optimization processes are underway.

3. Conclusions

We have investigated a new class of BDT-TPD-based copolymers. Preliminary results on the photovoltaic devices based on these materials revealed that the length of the alkyl chain on the TPD unit can modify the morphology of the copolymers/[60]PCBM blends. A PCE of 5.2% has been obtained for a thin layer of **P1**. Moreover, thick active layer BHJ solar cells have been studied and a PCE up to 3.8% was reached with **P1**. This result is among the highest PCE values reported so far for relatively thick films and could contribute to address issues related to roll-to-roll manufacturing processes of BHJ solar cells. Optimization of the fabrication of the photovoltaic devices is therefore underway to push forward the performances of these new copolymers. Finally, compounds **19** to **26** could be homopolymerized or copolymerized with new electron-rich comonomers to develop totally new well-defined photoactive and electroactive polymers.

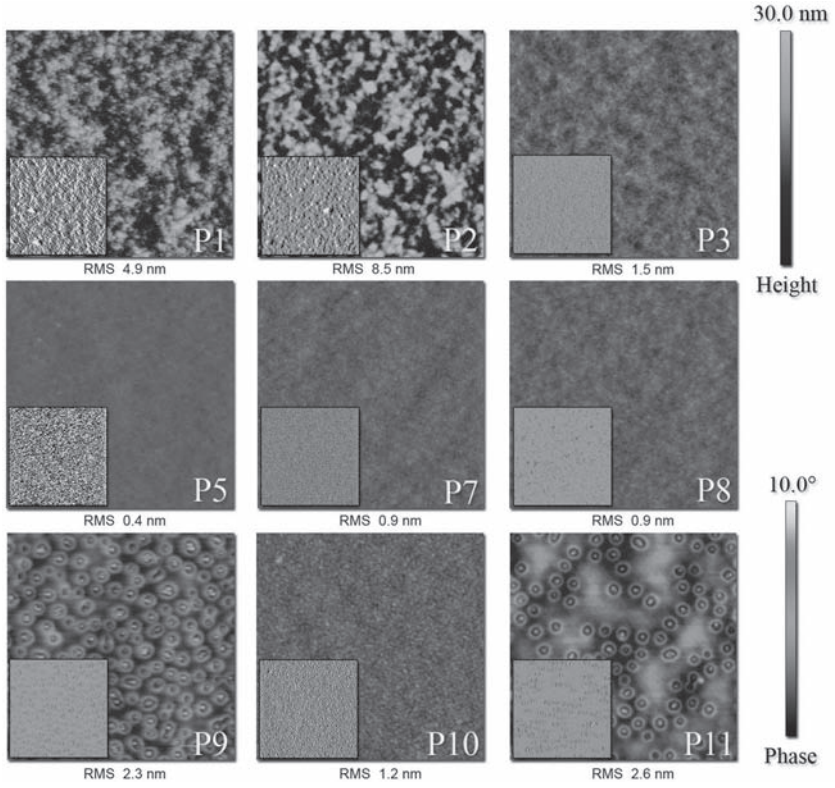

Figure 5. The AFM tapping mode height and simultaneously acquired phase insets images of poly(thieno[3,4-c]pyrrole-4,6-dione) derivatives (P1–P11, excepted P4 and P6). The scan size for height and phase images is 10 mm × 10 mm.

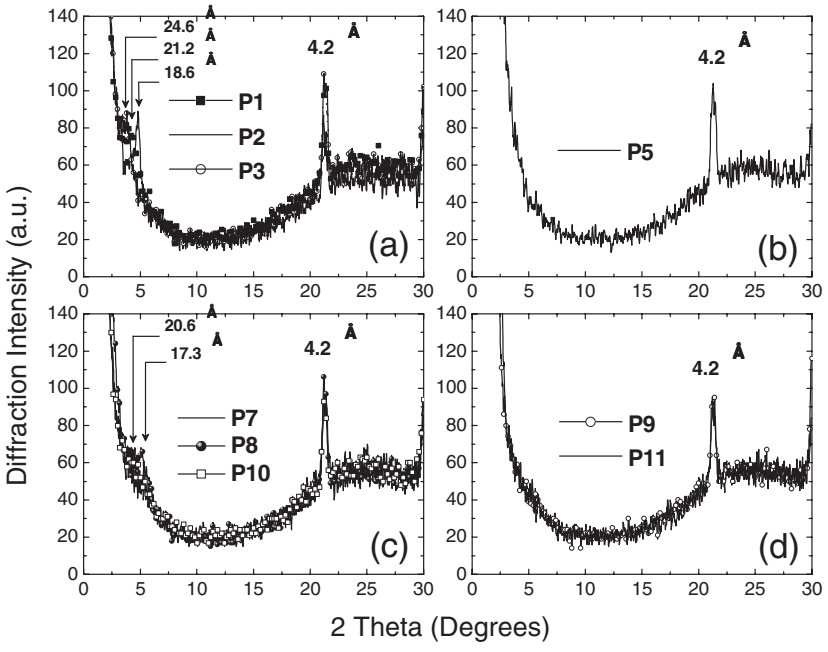

Figure 6. X-ray diffraction patterns of polymers P1 to P11-[60]PCBM blend films at room temperature.

4. Experimental Section

Instrumentation: ^{1}H and ^{13}C NMR spectra were recorded using a Varian AS400 or 300 in deuterated chloroform, dimethyl sulfoxide, or THF solution at 298 K. Number-average (M_n) and weight-average (M_w) molecular weights were determined by size exclusion chromatography (SEC) using a high temperature Varian Polymer Laboratories GPC220 equipped with a refractive index (RI) detector and a PL BV400 HT Bridge Viscometer. The column set consists of 2 PLgel Mixed C (300 mm × 7.5 mm) columns and a PLgel Mixed C guard column. The flow rate was fixed at 1.0 mL min^{-1} using 1,2,4-trichlorobenzene (TCB) (with 0.0125% BHT w/v) as the eluent. The temperature of the system was set to 140 °C. The sample was prepared at concentration of nominally 1.0 mg mL^{-1} in hot TCB. Dissolution was performed using a Varian Polymer Laboratories PL-SP 260VC sample preparation system. The sample vial was held at 160 °C with shaking for 1 h for complete dissolution. The solution was filtered through a 2 µm porous stainless steel filter used with the SP260 pipettor into a 2 mL chromatography vial. The calibration method used to generate the reported data was the classical polystyrene method using polystyrene narrow standards Easi-Vials PS-M from Varian Polymer Laboratories, which were dissolved in TCB. TGA measurements were carried out using a Mettler Toledo TGA SDTA 851e apparatus (heating rate of 20 °C min^{-1} under nitrogen flow) and the temperature of degradation (T_d) corresponds to a 5% weight loss. Differential scanning calorimetry (DSC) analysis was performed on a Perkin-Elmer DSC-7 instrument, calibrated with ultrapure indium. Glass transition temperature (T_g) was determined using a scanning rate of 20 °C min^{-1} under a nitrogen flow. UV-vis-NIR absorption spectra were recorded using a Varian Cary 500 UV-vis-NIR spectrophotometer with path length quartz cells of 1 cm. Spin-coated films on glass plates were used for solid-state UV-vis-NIR measurements. Optical bandgaps were determined from the onset of the absorption band. Cyclic voltammograms (CV) were recorded on a Solartron 1287 potentiostat using platinum wires as working electrode and counter-electrode at a scan rate of 50 mV s^{-1}. The reference electrode was Ag/Ag^{+} (0.1 M of $AgNO_3$ in acetonitrile) and the electrolyte was a solution of 0.1 M of tetrabutylammonium tetrafluoborate in dry acetonitrile. In these conditions, the oxidation potential of ferrocene was 0.09 V versus Ag/Ag^{+}, whereas the oxidation potential of ferrocene was 0.41 V versus saturated calomel electrode (SCE). The HOMO and LUMO energy levels were determined from the oxidation and reduction onsets (where the current differs from the baseline) assuming that SCE electrode is –4.7 eV from vacuum. The operation power was 40 kV, 30 mA and the collimator was 0.8 mm in diameter. GIXS experiments were performed using a Siemens D5000 X-ray diffractometer with a CuKα radiation source (1.540598 Å). The operation power was 40 kV, 30 mA. The surface topographies of BHJ active layers composed of donor polymers and [60]PCBM were obtained using AFM in tapping mode (Dimension V SPM, Veeco). The Si AFM tip was

used with a force constant of 42 N m^{-1} and AFM images were collected in air under ambient conditions.

Chemicals: Thiophene-3,4-dicarboxylic acid was purchased from Frontier Scientific. 2-(Tributylstannyl)thiophene was purchased from Aldrich. THF was distilled over a potassium/benzophenone system. Toluene and acetonitrile were distilled over calcium hydride before use. Synthesis of 5-octylthieno[3,4-c]pyrrole-4,6-dione[14] (**1**), 1,3-dibromo-5-octyl-thieno[3,4-c]pyrrole-4,6-dione[14] **(4)**, 2-trimethyltin thiophene **(7)**, 2-(trimethyltin)-3-octylthiophene[26] **(8)**, 2-(trimethyltin)-4-octylthiophene[27] **(10),** and 2,6-bis(trimethyltin)-4,8-di(2-ethylhexyloxyl)benzo[1,2-b:3,4-b]dithiophene[14] **(27)** were prepared according to procedures reported in literature. All the monomers were carefully purified prior to use in the polymerization reaction.

*Synthesis of 5-(2-ethylhexyl)thieno[3,4-c]pyrrole-4,6-dione **(2)***: A solution of thiophene-3,4-dicarboxylic acid (0.90 g, 5.23 mmol) in 21 mL of acetic anhydride was stirred at 140 °C overnight. The solvent was removed and the crude product was used for the next step without any purification. The brown solid (assuming 5.23 mmol) was dissolved into 55 mL of toluene and then 2-ethylhexylamine (1.02 g, 7.85 mmol) was added. The reaction mixture was refluxed for 24 h. The reaction mixture was cooled down and the solvent was removed under reduced pressure. The resulting solid was dissolved into 68 mL of thionyl chloride. The mixture was refluxed for 3 h then cooled. The solvent was removed under reduced pressure and the crude product was purified by column chromatography using dichloromethane:hexanes as the eluent (ratio 1:1) to afford 0.90 g of the product as a white solid (Y = 65%).

^{1}H NMR (400 MHz, $CDCl_3$, δ): 7.78 (s, 2H); 3.48 (d, 2H, J = 7.3 Hz); 1.76 (t, 1H, J = 6.1 Hz); 1.32–1.24 (m, 8H); 0.87 (t, 6H, J = 7.4 Hz).

^{13}C NMR (100 MHz, $CDCl_3$, δ): 163.16; 136.81; 125.71; 42.54; 38.35; 30.67; 28.67; 24.00; 23.23; 14.30; 10.62.

*Synthesis of 5-(dodecyl)thieno[3,4-c]pyrrole-4,6-dione **(3)***: This compound was synthesized as described for **2** using thiophene-3,4-dicarboxylic acid (10.00 g, 58.08 mmol) and 1-dodecylamine (16.14 g, 87.12 mmol) to afford 10.27 g of the product as a white solid (Y = 55%).

^{1}H NMR (400 MHz, $CDCl_3$, δ): 7.80 (s, 2H); 3.60 (t, 2H, J = 7.3 Hz); 1.65–1.62 (m, 2H); 1.30–1.24 (m, 18H); 0.87 (t, 3H, J = 6.5 Hz).

^{13}C NMR (100 MHz, $CDCl_3$, δ): 162.92; 136.91; 125.71; 38.75; 32.15; 29.87; 29.85; 29.81; 29.75; 29.59; 29.45; 28.72; 27.12; 22.93; 14.39.

*Synthesis of 1,3-dibromo-5-(2-ethylhexyl)thieno[3,4-c]pyrrole-4,6-dione **(5)***: 5-(2-ethylhexyl)-thieno[3,4-c]pyrrole-4,6-dione (0.45 g, 1.70 mmol) was dissolved in a mixture of sulfuric acid (2.6 mL) and trifluoroacetic acid (8.7 mL). The solution was kept in the dark. *N*-Bromosuccinimide (0.94 g, 5.28 mmol) was added in four portions and the reaction mixture was stirred at room temperature overnight. The brown-red solution was poured into water and extracted twice with dichloromethane. The organic phases were combined and dried over anhydrous magnesium sulphate. The solvent was removed under reduced pressure and the crude product was purified by column chromatography using dichloromethane:hexanes as the eluent (ratio 3:2) to afford 1.00 g of the product as white powder (Y = 78%).

^{1}H NMR (400 MHz, $CDCl_3$, δ): 3.49 (d, 2H); 1.8 (m, 1H); 1.34–1.27 (m, 8H); 0.89 (t, 6H, J = 7.1 Hz).

^{13}C NMR (100 MHz, $CDCl_3$, δ):160.92; 134.95; 113.18; 42.86; 38.40; 30.74; 28.77; 24.05; 23.18; 14.32; 10.60.

*Synthesis of 1,3-dibromo-5-(dodecyl)thieno[3,4-c]pyrrole-4,6-dione **(6)***: This compound was synthesized as described for **5** using 5-(dodecyl)-thieno[3,4-c]pyrrole-4,6-dione (3.00 g, 9.32 mmol), a mixture of sulfuric acid (17.4 mL) and trifluoroacetic acid (56.4 mL), and *N*-bromosuccinimide (4.44 g, 24.94 mmol) to afford 3.03 g of the product as white powder (Y = 68%).

^{1}H NMR (400 MHz, $CDCl_3$, δ): 3.59 (t, 2H, J = 7.2 Hz); 1.64–1.61 (m, 2H); 1.30–1.25 (m, 18H); 0.87 (t, 3H, J = 6.5 Hz).

^{13}C NMR (100 MHz, $CDCl_3$, δ): 160.63; 135.03; 113.17; 39.08; 32.16; 29.86; 29.84; 29.81; 29.69; 29.59; 29.40; 28.50; 27.04; 22.94; 14.38.

*Synthesis of 2-(trimethyltin)-3-ethylthiophene **(9)***: *n*-Butyllithium (2.5 M in hexane) (27.60 mmol, 11.0 mL) was added dropwise to a solution of 2-bromo-3-ethylthiophene (5.00 g, 26.17 mmol) in dry THF (50 mL) at −78 °C. The solution was stirred at −78 °C for 2 h. Then, trimethyltin chloride (39.40 mmol, 40.0 mL) was added at once to the reaction mixture. The cooling bath was removed and the reaction was warmed to room temperature overnight. The reaction mixture was then poured into hexanes. The organic phase was washed with water then brine. The solvent was removed under reduced pressure and the crude product (brownish oil) was purified by distillation under high vacuum to afford 4.57 g of the product as a colorless oil (Y = 63%) (boiling point 73–75 °C at 0.35 mmHg).

^{1}H NMR (300 MHz, $CDCl_3$, δ): 7.55 (d, 1H, J = 4.6 Hz); 7.13 (d, 1H, J = 4.7 Hz); 2.68 (q, 2H, J = 7.7 Hz); 1.24 (t, 3H, J = 7.5 Hz); 0.39 (s, 9H).

*Synthesis of 1,3-di(thien-2'-yl)-5-octylthieno[3,4-c]pyrrole-4,6-dione **(11)***: Compound **4** (2.10 g, 4.96 mmol) was dissolved into dry THF (200 mL). 2-(tributylstannyl)thiophene (15.00 mmol, 4.76 mL), and bis(triphenylphosphine) palladium(II) dichloride (210 mg, 6%) were added to the reaction mixture. The solution was refluxed for 24 h then cooled and poured into water. The mixture was extracted twice with dichloromethane. The organic phases were combined, washed with brine, and dried over anhydrous magnesium sulphate. The solvent was removed under reduce pressure and the crude product was purified by column chromatography using dichloromethane:hexanes as the eluent (ratio 1:1) to afford 1.60 g of the product as a green powder (Y = 75%).

^{1}H NMR (400 MHz, d^8-THF, δ): 8.33 (d, 2H); 7.78 (d, 2H); 7.34 (t, 2H, J = 4.2 Hz); 3.83 (t, 2H, J = 7.1 Hz); 1.89 (m, 2H); 1.53–1.47 (m, 10H); 1.05 (t, 3H, J = 7.2 Hz).

^{13}C NMR (100 MHz, d^8-THF, δ): 162.08; 135.71; 132.57; 130.09; 129.12; 128.94; 128.42; 38.14; 32.00; 29.36; 28.48; 26.99; 22.73; 13.62. One peak is missing due to the deuterated solvent.

*Synthesis of 1,3-di(thien-2'-yl)-5-(2-ethylhexyl)thieno[3,4-c]pyrrole-4,6-dione **(12)***: This compound was synthesized as described for **11** using **5** (2.10 g, 4.96 mmol), dry THF (100 mL), 2-(tributylstannyl)thiophene (15.00 mmol, 4.76 mL), and bis(triphenylphosphine) palladium(II) dichloride (210 mg, 6%) to afford 1.90 g of the product as a green powder (Y = 89%).

^{1}H NMR(400 MHz, $CDCl_3$, δ): 8.03 (d, 2H, J = 3.1 Hz); 7.44 (d, 2H, J = 4.6 Hz); 7.13 (t, 2H, J = 4.0 Hz); 3.58 (d, 2H, J = 7.3 Hz); 1.87–1.84 (m, 1H); 1.46–1.26 (m, 8H); 0.94–0.88 (m, 6H).

^{13}C NMR(100 MHz, $CDCl_3$, δ): 163.17; 136.72; 132.68; 130.15; 128.87; 128.69; 128.65; 42.75; 38.49; 30.83; 28.84; 24.14; 23.28; 14.33; 10.70.

*Synthesis of 1,3-di(thien-2'-yl)-5-dodecylthieno[3,4-c]pyrrole-4,6-dione **(13)***: This compound was synthesized as described for **11** using **6** (1.00 g, 2.09 mmol), dry THF (50 mL), 2-(tributylstannyl)thiophene (4.18 mmol, 1.45 mL), and bis(triphenylphosphine) palladium(II) dichloride (73 mg, 6%) to afford 0.82 g of the product as a yellow green powder (Y = 82%).

^{1}H NMR (400 MHz, $CDCl_3$, δ): 8.01 (d, 2H, J = 3.0 Hz); 7.45 (d, 2H, J = 0.6 Hz); 7.13 (t, 2H, J = 1.0 Hz); 3.66 (t, 2H, J = 7.3 Hz); 1.70–1.65 (m, 2H); 1.37–1.25 (m, 18H); 0.95 (t, 3H, J = 7.3 Hz).

^{13}C NMR (100 MHz, $CDCl_3$, δ): 162.87; 136.73; 132.68; 130.11; 128.89; 128.67; 128.63; 38.83; 32.16; 29.91; 29.88; 29.83; 29.74; 29.60; 29.48; 28.73; 27.20; 22.94; 14.39.

*Synthesis of 1,3-di(3'-octylthien-2'-yl)-5-octylthieno[3,4-c]pyrrole-4,6-dione **(14)***: This compound was synthesized as described for **11** using **4** (1.26 g, 2.98 mmol), dry THF (100 mL), 2-(trimethyltin-3-octylthiophene) **(8)** (7.45 mmol, 3.58 g), and bis(triphenylphosphine) palladium(II) dichloride (210 mg, 6%). The crude product was purified by column chromatography using dichloromethane:hexanes as the eluent (ratio 3:2) to afford 1.52 g of the product as a sticky oil (Y = 79%).

^{1}H NMR (400 MHz, $CDCl_3$, δ): 7.42 (d, 2H, J = 5.2 Hz); 7.02 (d, 2H, J = 5.2 Hz); 3.63 (t, 2H, J = 7.2 Hz); 2.80 (t, 4H, J = 7.9 Hz); 1.66–1.63 (m, 6H); 1.30–1.25 (m, 30H); 0.88 (t, 9H, J = 6.4 Hz).

^{13}C NMR (100 MHz, $CDCl_3$, δ): 162.55; 144.55; 137.25; 130.83; 130.06; 127.83; 125.27; 38.69; 32.11; 32.04; 30.77; 29.89; 29.77; 29.64; 29.50; 29.43; 29.40; 28.69; 27.19; 22.90; 22.87; 14.34; 14.33.

*1,3-di(3'-ethylthien-2'-yl)-5-octylthieno[3,4-c]pyrrole-4,6-dione **(15)***: This compound was synthesized as described for **11** using **4** (0.97 g; 22.90 mmol), dry THF (60 mL), 2-(trimethyltin)-3-ethylthiophene **(9)** (1.89 g; 69.00 mmol), and bis(triphenylphosphine) palladium(II) dichloride (96 mg, 6%) to afford 0.75 g of the product as a sticky orange oil (Y = 68%).

^{1}H NMR (300 MHz, $CDCl_3$, δ): 7.42 (d, 2H, J = 5.2 Hz); 7.05 (d, 2H, J = 5.2Hz); 3.06 (t, 2H, J = 7.2Hz); 2.82 (q, 4H, J = 7.5Hz); 1.67–1.59 (m, 2H); 1.28 (m, 16H); 0.86 (t, 3H, J = 6.3Hz).

^{13}C NMR (75 MHz, $CDCl_3$, δ): 162.33; 145.55; 137.04; 130.71; 129.35; 127.76; 124.63; 38.47; 31.80; 29.18(2C); 28.48; 26.95; 22.91; 22.65; 14.79; 14.10.

Synthesis of 1,3-di(4'-octylthien-2'-yl)-5-octylthieno[3,4-c]pyrrole-4,6-dione ***(16)***: This compound was synthesized as described for **11** using **4** (1.00 g, 2.36 mmol), dry THF (50 mL) 2-(trimethyltin)-4-octylthiophene **(10)** (1.87 g; 5.20 mmol), and bis(triphenylphosphine) palladium(II) dichloride (9.9 mg, 6%) to afford 0.55 g of the product as a sticky orange oil (Y = 36%).

^{1}H NMR (400 MHz, $CDCl_3$, δ): 7.87 (s, 2H); 7.02 (s, 2H); 3.65 (t, 2H, J = 7.4 Hz); 2.26 (t, 4H, J = 7.6 Hz); 1.67–1.61 (m, 6H); 1.33–1.29 (m, 30H); 0.89 (t, 9H, J = 6.5 Hz).

^{13}C NMR (100 MHz, $CDCl_3$, δ):162.94; 145.18; 137.02; 132.38; 131.32; 128.28; 123.77; 38.83; 32.13; 30.70; 29.65; 29.52; 29.49; 29.43; 28.80; 27.24; 22.93; 14.37. Some peaks are missing due to overlapping.

Synthesis of 1,3-di(3'-octylthien-2'-yl)-5-dodecylthieno[3,4-c]pyrrole-4,6-dione ***(17)***: This compound was synthesized as described for **11** using **6** (0.95 g, 1.98 mmol), dry THF (46 mL), 2-(trimethyltin)-3-octylthiophene) **(8)** (4.35 mmol, 1.56 g), and bis(triphenylphosphine) palladium(II) dichloride (8.3 mg, 6%). The crude product was purified by column chromatography using dichloromethane:hexanes as the eluent (ratio 2:3) to afford 0.96 g of the product as a yellow solid (Y = 68%).

^{1}H NMR (400 MHz, $CDCl_3$, δ): 7.46 (d, 2H, J = 5.1 Hz); 7.04 (d, 2H, J = 5.2 Hz); 3.64 (t, 2H, J = 7.2 Hz); 2.86 (t, 4H, J = 7.7 Hz); 1.70–1.59 (m, 6H); 1.31–1.25 (m, 38H); 0.86 (t, 9H, J = 3.9 Hz).

^{13}C NMR (100 MHz, $CDCl_3$, δ): 167.24; 145.19; 131.58; 130.30; 130.04; 128.31; 112.99; 38.64; 31.90; 31.79; 30.56; 29.50; 29.40; 29.27; 29.17; 26.95; 22.68; 22.62; 14.10; 14.07. Some peaks are missing due to overlapping.

Synthesis of 1,3-di(4'-octylthien-2'-yl)-5-dodecylthieno[3,4-c]pyrrole-4,6-dione ***(18)***: This compound was synthesized as described for **11** using **6** (0.91 g, 1.90 mmol), dry THF (45 mL), 2-(trimethyltin)-4-octylthiophene **(10)** (1.5 g, 4.17 mmol), and bis(triphenylphosphine) palladium(II) dichloride (8.0 mg, 6% mol). The crude product was purified by column chromatography using dichloromethane:hexanes as the eluent (ratio 2:3) to afford 0.73 g of the product as a yellow wax (Y = 75%).

^{1}H NMR (400 MHz, $CDCl_3$, δ): 7.87 (s, 2H); 7.01 (s, 2H); 3.65 (t, 2H, J = 7.3 Hz); 2.62 (t, 4H, J = 7.6 Hz); 1.65–1.61 (m, 6H); 1.33–1.25 (m, 38H); 0.88 (t, 9H, J = 4.9 Hz).

^{13}C NMR (100 MHz, $CDCl_3$, δ): 162.91; 145.17; 136.99; 132.38; 131.31; 128.27; 123.74; 38.83; 32.17; 32.13; 30.70; 30.66; 29.89; 29.84; 29.77; 29.66; 29.60; 29.57; 29.53; 28.80; 27.25; 22.93; 14.37. Some peaks are missing due to overlapping.

Synthesis of 1,3-di(2'-bromothien-5'-yl)-5-octylthieno[3,4-c]pyrrole-4,6-dione ***(19)***: Compound **11** (0.86 g, 2.00 mmol) was dissolved in a mixture of acetic acid and chloroform (60 mL) (ratio 1:1). The solution was cooled to 0 °C and kept in the dark. *N*-Bromosuccinimide (0.79 g, 4.43 mmol) was added to the solution in several portions. The cooling bath was removed and the reaction was stirred at ambient temperature for 24 h. The reaction solution was poured into water and extracted several times with chloroform. The organic phases were combined, washed with brine, and dried over anhydrous magnesium sulphate. The solvent was removed under reduced pressure and the crude product was purified by column chromatography using dichloromethane:hexanes as the eluent (ratio 1:1) to afford 1.16 g of the product as a bright yellow solid (Y = 99%).

^{1}H NMR (400 MHz, $CDCl_3$, δ): 7.65 (d, 2H, J = 4 Hz); 7.09 (d, 2H, J = 4 Hz); 3.64 (t, 2H, J = 6.9 Hz); 1.67 (m, 2H); 1.32–1.26 (m, 10H); 0.87 (t, 3H, J = 5.4 Hz).

^{13}C NMR (100 MHz, $CDCl_3$, δ): 162.54; 135.32; 133.96; 131.37; 129.97; 128.83; 116.98; 38.93; 32.03; 29.41(2C); 28.69; 27.20; 22.87; 14.34.

Synthesis of 1,3-di(2'-bromothien-5'-yl)-5-(2-ethylhexyl)thieno[3,4-c]pyrrole-4,6-dione ***(20)***: This compound was synthesized as described for **19** using **12** (1.29 g, 3.00 mmol), a mixture of acetic acid and chloroform (60 mL) (ratio 1:1) at 0 °C, and *N*-bromosuccinimide (1.20 g, 6.67 mmol). The crude product was purified by gradient column chromatography using hexanes to dichloromethane:hexanes (ratio 1:1 to 2:3) to afford 1.72 g of the product as a bright yellow solid (Y = 98%).

^{1}H NMR (400 MHz, $CDCl_3$, δ): 7.65 (d, 2H, J = 4.0 Hz); 7.07 (d, 2H, J = 4.0 Hz); 3.54 (d, 2H, J = 7.3 Hz); 1.82 (t, 1H, J = 6.0 Hz); 1.38–1.29 (m, 8H); 0.92 (t, 6H, J = 2.9 Hz).

^{13}C NMR (100 MHz, $CDCl_3$, δ): 162.92; 135.37; 133.96; 131.38; 130.01; 128.79; 116.98; 42.87; 38.51; 30.83; 28.86; 28.83; 24.13; 23.28; 14.34.

Synthesis of 1,3-di(2'-bromothien-5'-yl)-5-dodecylthieno[3,4-c]pyrrole-4,6-dione ***(21)***: This compound was synthesized as described for **19** using **13** (0.80 g, 1.65 mmol), a mixture of acetic acid and chloroform (40 mL) (ratio 1:1) at 0 °C, and *N*-bromosuccinimide (0.65 g, 3.62 mmol). The crude product was purified by column chromatography using dichloromethane:hexanes as the eluent (ratio 1:1) to afford 0.80 g of the product as a yellow solid (Y = 76%).

^{1}H NMR (400 MHz, $CDCl_3$, δ): 7.65 (d, 2H, J = 4.0 Hz); 7.08 (d, 2H, J = 4.0 Hz); 3.64 (t, 2H, J = 7.3 Hz); 1.66 (m, 2H); 1.32–1.25 (m, 18H); 0.87 (t, 3H, J = 6.5 Hz).

^{13}C NMR (100 MHz, $CDCl_3$, δ): 162.63; 135.39; 133.96; 131.39; 129.99; 128.87; 116.97; 38.95; 32.16; 31.20; 29.87; 29.81; 29.72; 29.60; 29.45; 28.69; 27.18; 22.94; 14.28.

Synthesis of 1,3-di(5'-bromo-3-octylthien-2'-yl)-5-octylthieno[3,4-c]pyrrole-4,6-dione ***(22)***: This compound was synthesized as described for **19** using **14** (1.10 g, 1.72 mmol), a mixture of acetic acid and chloroform (50 mL) (ratio 1:1) at 0 °C, and *N*-bromosuccinimide (0.68 g, 3.76 mmol). After the addition of NBS, the cooling bath was removed and the reaction was stirred at ambient temperature for 24 h. The solution was then heated up to 55 °C for 24 h. The reaction was carefully monitored by thin layer chromatography (TLC). The reaction mixture was cooled and poured into water. The mixture was extracted three times using chloroform. The chloroform parts were combined, washed with brine, and dried over anhydrous magnesium sulphate. The crude product was purified by column chromatography using dichloromethane:hexanes as the eluent (ratio 1:1) to afford 1.30 g of the product as a yellow solid (Y = 82%).

^{1}H NMR (400 MHz, $CDCl_3$, δ): 6.96 (s, 2H); 3.60 (t, 2H, J = 7.1 Hz); 2.75- 2.71 (t, 4H, J = 7.6 Hz); 1.64–1.60 (m, 6 H); 1.30–1.25 (m, 30 H); 0.88–0.84 (t, 9H, J = 5.7 Hz).

^{13}C NMR (100 MHz, $CDCl_3$, δ): 162.26; 145.13; 135.63; 132.81; 130.94; 126.63; 115.69; 38.78; 32.11; 32.04; 30.57; 30.06; 29.73; 29.61; 29.49; 29.42(2C); 28.68; 27.19; 22.92; 22.89; 14.35; 14.32.

Synthesis of 1,3-di(5'-bromo-3'-ethylthien-2'-yl)-5-octylthieno[3,4-c]pyrrole-4,6-dione ***(23)***: This compound was synthesized as described for **22** using **15** (0.36 g, 0.75 mmol), a mixture of acetic acid and chloroform (24 mL) (ratio 1:1) at 0 °C, and *N*-bromosuccinimide (0.29 g, 1.65 mmol) to afford 0.32 g of the product as a highly viscous orange oil (Y = 66%).

^{1}H NMR (300 MHz, $CDCl_3$, δ): 7.01 (s, 2H); 3.61 (t, 2H, J = 7.4 Hz); 2.7 (q, 4H, J = 7.5 Hz); 1.66–1.60 (m, 2H); 1.28–1.23 (m, 16H); 0.87 (t, 3H, J = 6.2 Hz).

^{13}C NMR (75 MHz, $CDCl_3$, δ): 162.07; 146.13; 135.42; 132.19; 130.83; 126.08; 115.53; 38.58; 31.79; 29.17(2C); 28.45; 26.95; 23.09; 22.65; 14.61; 14.11.

Synthesis of 1,3-di(5'-bromo-4'-octylthien-2'-yl)-5-octylthieno[3,4-c]pyrrole-4,6-dione ***(24)***: This compound was synthesized as described for **22** using **16** (0.55 g, 0.85 mmol), a mixture of acetic acid and chloroform (20 mL) (ratio 1:1) at 0 °C, and *N*-bromosuccinimide (0.29 g, 1.65 mmol) to afford 0.52 g of the product as a yellow solid (Y = 72%).

^{1}H NMR (400 MHz, $CDCl_3$, δ): 7.60 (s, 2H); 3.61 (t, 2H, J = 7.1 Hz); 2.54 (t, 4H, J = 7.5 Hz); 1.66–1.60 (m, 6H); 1.33–1.28 (m, 30H); 0.87 (t, 9H, J = 6.6 Hz).

^{13}C NMR (100 MHz, $CDCl_3$, δ): 162.61; 143.96; 135.62; 132.09; 130.47; 128.49; 113.76; 38.91; 32.13; 29.96; 29.89; 29.75; 29.61; 29.52; 29.46; 28.76; 27.25; 22.93; 14.38. Some peaks are missing due to overlapping.

Synthesis of 1,3-di(5'-bromo-3'-octylthien-2'-yl)-5-dodecylthieno[3,4-c]pyrrole-4,6-dione ***(25)***: This compound was synthesized as described for **22** using **17** (1.47 g, 2.07 mmol), a mixture of acetic acid and chloroform (50 mL) (ratio 1:1) at 0 °C, and *N*-bromosuccinimide (0.82 g, 4.55 mmol) to afford 1.26 g of the product as a yellow solid (Y = 70%).

^{1}H NMR (400 MHz, $CDCl_3$, δ): 6.98 (s, 2H); 3.61 (t, 2H, J = 7.2 Hz); 2.74 (t, 4H, J = 7.8 Hz); 1.64–1.58 (m, 6H); 1.30–1.26 (m, 38H); 0.87 (t, 9H, J = 6.4 Hz).

^{13}C NMR (100 MHz, $CDCl_3$, δ): 162.34; 145.17; 135.69; 132.84; 130.97; 126.55; 115.68; 38.81; 32.10; 32.03; 30.59; 30.03; 29.71; 29.60; 29.47; 29.42; 29.40; 28.67; 27.18; 22.90; 22.87; 14.35. Some peaks are missing due to overlapping.

Synthesis of 1,3-di(5'-bromo-4'-octylthien-2'-yl)-5-dodecylthieno[3,4-c] pyrrole-4,6-dione ***(26)***: This compound was synthesized as described for **22** using **18** (0.60 g, 0.85 mmol), a mixture of acetic acid and chloroform (20 mL) (ratio 1:1) at 0 °C, and *N*-bromosuccinimide (0.29 g, 1.65 mmol) to afford 0.45 g of the product as a yellow solid (Y = 65%).

^{1}H NMR (400 MHz, $CDCl_3$, δ): 6.98 (s, 2H); 3.61 (t, 2H, J = 7.2 Hz); 2.74 (t, 4H, J = 7.8 Hz); 1.64–1.58 (m, 6H); 1.30–1.26 (m, 38H); 0.87 (t, 9H, J = 6.4 Hz).

^{13}C NMR (100 MHz, $CDCl_3$, δ): 162.61;143.95; 135.63; 132.09; 130.46; 128.50; 113.76; 38.92; 32.17; 32.13; 29.97; 29.89; 29.84; 29.77; 29.61; 29.52; 28.76; 27.25; 22.95; 22.94; 14.38. Some peaks are missing due to overlapping.

Representative procedure for polymerization: 2,6-Bis(trimethyltin)-4,8-di(2-ethylhexyloxyl)-benzo[1,2-b:3,4-b]dithiophene ***(27)***: (0.5 mmol), compounds **(4–6; 19–26)** (0.5 mmol), $Pd_2(dba)_3$ (2 mol%), and P(o-Tol)$_3$ (8 mol%) were put in a round bottom flask (25 mL). The system was then purged three times by vacuum/argon cycling. The solids were dissolved in 16 mL of dry and oxygen free toluene. The temperature was increased from room temperature to 110 °C using an oil bath equipped with a temperature controller. After 24 to 36 h of polymerization time, 100 µL of bromobenzene was added to the viscous reaction mixture as an end-capping agent. After an additional hour of reaction, 100 µL of trimethyltin phenyl was added to complete the end capping procedure. After an additional hour of reaction, the whole mixture was cooled to room temperature and poured in 500 mL of cold methanol. The precipitate was filtered. Soxhlet extraction with acetone followed by hexane removed catalyst residues and low molecular weight material. Polymers were then extracted with chloroform. The solvent was reduced to about 30 mL and the mixture was poured into cold methanol. Polymers were recovered by filtration and further purification was done to remove all metals impurities. Typical yields from 80 to 95% were obtained.

Photovoltaic devices: The bulk heterojunction photovoltaic solar cell were fabricated using the following structure: glass/ITO/PEDOT:PSS/polymer:[60]PCBM/Al as illustrated in the Figure 1. Commercial ITO (ITO-coated glass substrate (25 × 25 mm^2)) with a sheet resistance of ≤10 Ohms per sq (Thin Film Devices Inc, USA) were cleaned using following sequence in an ultrasonic bath: detergent, water, acetone, and 2-propanol. After treatments in plasma-O_2 for 5 min, each ITO substrate was patterned using photolithography techniques. Then PEDOT:PSS, (Baytron P, H. C. Starck) was spin-coated (2000 rpm, 60 s) on the ITO surface and dried at 120 °C for 1 h. After cooling the substrate, an oDCB solution of polymer and [6,6]-phenyl-C_{61} butyric acid methyl ester ([60]PCBM) (Nano-C, USA) mixture (1:2, wt/wt) was spin-coated. The substrates were then put in a thermal evaporation chamber in order to evaporate 70 nm of the aluminum layer (0.2–0.3 nm s^{-1}) under high vacuum (2×10^{-5} torr) through a shadow mask (active area 25 mm^2). The current–voltage characteristics of the photovoltaic cells were measured using a Kheithey 2400 (*I*–*V*) Digital SourceMeter under a collimated beam. The measurements were conducted under the irradiation of AM 1.5G filter (No 81094) simulated solar light (100 mW cm^{-2}) by using a 150 W Oriel Instruments Solar Simulator and xenon lamp. Light intensity was adjusted using a Gentec-eo power detector (PS-330).

Acknowledgements

This work was supported by grants from NSERC, a research contract from the Sustainable Development Technology Canada (SDTC) program, and a research contract from Defence Research and Development Canada (DRDC), Valcartier, Qc, Canada. A special thanks to Sheila Rodman from Konarka Technologies Inc. for the molecular weight measurements.

Received: August 26, 2010
Revised: October 4, 2010
Published online: December 22, 2010

[1] S. Günes, H. Neugebauer, N. S. Sariciftci, *Chem. Rev.* **2007**, *107*, 1324.
[2] K. M. Coakley, M. D. McGehee, *Chem. Mater.* **2004**, *16*, 4533.
[3] *Organic Photovoltaics: Materials, Device Physics, and Manufacturing Technologies*, (Eds: C. J. Brabec, V. Dyakonov, U. Scherf), Wiley-VCH, Weinheim , Germany **2008**.
[4] G. Li, V. Shrotriya, J. Huang, Y. Yao, T. Moriarty, K. Emery, Y. Yang, *Nat. Mater.* **2005**, *4*, 864.
[5] J. Y. Kim, S. H. Kim, H. H. Lee, K. Lee, W. Ma, X. Gong, A. J. Heeger, *Adv. Mater.* **2006**, *18*, 572.
[6] K. Kim, J. Liu, M. A. G. Namboothiry, D. L. Carroll, *Appl. Phys. Lett.* **2007**, *90*, 163511.
[7] M. Al-Ibrahim, H.-K. Roth, U. Zhokhavets, G. Gobsch, S. Sensfuss, *Sol. Energy Mater. Sol. Cells* **2005**, *85*, 13.
[8] B. C. Thompson, J. M. J. Fréchet, *Angew. Chem. Int. Ed.* **2008**, *47*, 58.
[9] M. C. Scharber, D. Mühlbacher, M. Koppe, P. Denk, C. Waldauf, A. J. Heeger, C. J. Brabec, *Adv. Mater.* **2006**, *18*, 789.
[10] J. Peet, J. Y. Kim, N. E. Coates, W. L. Ma, D. Moses, A. J. Heeger, G. C. Bazan, *Nat. Mater.* **2007**, *6*, 497.
[11] S. H. Park, A. Roy, S. Beaupré, S. Cho, N. Coates, J. S. Moon, D. Moses, M. Leclerc, K. Lee, A. J. Heeger, *Nat. Photonics* **2009**, *3*, 297.
[12] E. Zhou, J. Cong, S. Yamakawa, Q. Wei, M. Nakamura, K. Tajima, C. Yang, K. Hashimoto, *Macromolecules* **2010**, *43*, 2873.
[13] Solarmer homepage, www.solarmer.com (accessed November 2010).
[14] Y. Zou, A. Najari, P. Berrouard, S. Beaupré, B. R. Aïch, Y. Tao, M. Leclerc, *J. Am. Chem. Soc.* **2010**, *132*, 5330.
[15] Y. Zhang, S. K. Hau, H.-L. Yip, Y. Sun, O. Acton, A. K.-Y. Jen, *Chem. Mater.* **2010**, *22*, 2696.
[16] C. Piliego, T. W. Holcombe, J. D. Douglas, C. H. Woo, P. M. Beaujuge, J. M. J. Fréchet, *J. Am. Chem. Soc.* **2010**, *132*, 7595.
[17] G. Zhang, Y. Fu, Q. Zhang, Z. Xie, *Chem. Commun.* **2010**, *46*, 4997.
[18] M.-C. Yuan, M.-Y. Chiu, S.-P. Liu, C-M. Chen, K.-H. Wei, *Macromolecules* **2010**, *43*, 6936.
[19] Y. Liang, Z. Xu, J. Xia, S.-T. Tsai, Y. Wu, G. Li, C. Ray, L. Yu, *Adv. Mater.* **2010**, *22*, E135.
[20] C. B. Nielsen, T. Bjørnholm, *Org. Lett.* **2004**, *6*, 3881.
[21] W. Ma, C. Yong, X. Gong, K. Lee, A. J. Heeger, *Adv. Funct. Mater.* **2005**, *15*, 1617.
[22] A. L. Fahrenbrach, R. H. Bube, *Fundamentals of Solar Cells: Photovoltaics Solar Energy Conversion*, Academic Press, New York **1983**.
[23] H. C. Raus, *Solar Cell Array Design Handbook*, Van Nostrand Reinhold, New York **1980**, 56.
[24] A. Moliton, J.-M. Nunzi, *Polym. Int.* **2006**, *55*, 583.
[25] F. C. Krebs, *Sol. Energy Mater. Solar Cells.* **2009**, *93*, 394.
[26] J. Bras, S. Guillerez, B. Pépin-Donat, *Chem. Mater.* **2000**, *12*, 2372.
[27] N. Leclerc, A. Michaud, K. Sirois, J.-F. Morin, M. Leclerc, *Adv. Funct. Mater.* **2006**, *16*, 1694.